

Quantum quench of Kondo correlations in optical absorption

C. Latta^{1*}, F. Haupt¹, M. Hanl², A. Weichselbaum², M. Claassen¹, W. Wuester¹, P. Fallahi¹, S. Faelt¹, L. Glazman³, J. von Delft², H. E. Türeci^{4,1}, A. Imamoglu^{1*}

¹ Institute of Quantum Electronics, ETH-Zürich, CH-8093 Zürich, Switzerland,

² Arnold Sommerfeld Center for Theoretical Physics,

Ludwig-Maximilians-Universität München, D-80333 München, Germany,

³ Sloane Physics Laboratory, Yale University, New Haven, CT 06520, USA

⁴ Department of Electrical Engineering, Princeton University, Princeton, New Jersey 08544, USA

*To whom correspondence should be addressed;

E-mail: clatta@phys.ethz.ch or imamoglu@phys.ethz.ch

(Dated:)

The interaction between a single confined spin and the spins of a Fermionic reservoir leads to one of the most spectacular phenomena of many body physics – the Kondo effect[12, 13]. Here we report the observation of Kondo correlations in optical absorption measurements on a single semiconductor quantum dot tunnel-coupled to a degenerate electron gas. In stark contrast to transport experiments[17–19], absorption of a single photon leads to an abrupt change in the system Hamiltonian and a quantum quench of Kondo correlations. By inferring the characteristic power law exponents from the experimental absorption line-shapes, we find a unique signature of the quench in the form of an Anderson orthogonality catastrophe[15, 16], originating from a vanishing overlap between the initial and final many-body wave-functions. We also show that the power-law exponents that determine the degree of orthogonality can be tuned by applying an external magnetic field which gradually turns

the Kondo correlations off[23]. Our experiments demonstrate that optical measurements on single artificial atoms offer new perspectives on many-body phenomena previously studied exclusively using transport spectroscopy. Moreover, they initiate a new paradigm for quantum optics where many-body physics influences electric field and intensity correlations.

Optical spectroscopy of single quantum dots (QD) has demonstrated its potential for applications in quantum information processing, particularly in the realization of single and entangled photon sources[1, 2], coherent spin qubits[3, 4] and a spin-photon interface[5, 6]. Even though recent experiments have established this system as a new paradigm for solid-state quantum optics, all of the striking experimental observations to date could be understood within the framework of single- or few-particle physics enriched by perturbative coupling to reservoirs involving either phonons, a degenerate electron gas [7, 8], or nuclear spins [9, 10]).

We present differential transmission (DT)

experiments[11] on a single charge-tunable QD that reveal optical signatures of the Kondo effect[12, 13]. In contrast to prior experiments[8, 14], the tunnel coupling between the QD and a nearby degenerate electron gas, which we refer to as the Fermionic reservoir (FR), is engineered to be so strong that the resulting exchange interactions cannot be treated within the framework of a perturbative system-reservoir theory: In the initial state, the “system” (QD spin) is maximally entangled with the FR, forming a screened singlet.

The fundamentally new feature that differentiates the results we present from all prior transport based investigation of the Kondo effect[17–19], is the realization of a quantum quench of the local Hamiltonian; in our experiments, photon absorption abruptly turns the exchange interaction between the QD electron and the FR off, leading to the destruction of the correlated QD-FR singlet that otherwise acts as a local scattering potential for all FR electrons. As was shown by Anderson[15, 16], the overlap between N -electron FR states with and without a local scattering potential scales as $N^{-\alpha}$ with $\alpha > 0$. This reduced overlap, termed Anderson orthogonality catastrophe (AOC), leads to a power-law tail in absorption if the scattering potential is turned on or off by photon absorption. Here, we determine the AOC induced power-law exponents in absorption line shape that uniquely characterize the (quench of) Kondo correlations. Moreover, by tuning the applied laser frequency, we observe

both the perturbative and non-perturbative regimes of the Kondo effect in one absorption line shape, without having to change the FR (electron) temperature T_{FR} .

Experimental setup. The schematic of the QD sample we study is shown in Figure 1a: a gate voltage V_g applied between a top Schottky gate and the degenerate electron gas allows us to tune the charging state of the QD[20]. Figure 1B shows the photoluminescence (PL) spectrum as a function of V_g , where different discrete *charging plateaux* are clearly observable. In this paper we focus on the X^- plateau, for which the QD is single-electron charged and the influence of the FR on the QD PL dispersion and linewidth is strongest. The X^- optical transition couples the *initial configuration*, containing on average one electron in the QD, to a *final configuration*, containing on average two electrons and a valence-band hole (a negatively charged trion). This transition can be described within the framework of an excitonic Anderson model (EAM) [23, 24], depicted schematically in Fig. 2C (and described explicitly in Supporting Online Material). It is parameterized by the energy ε of the QD electron level w.r.t. to the Fermi level, the on-site Coulomb repulsion U_{ee} , the tunnel rate Γ between QD and FR, the half-bandwidth D of the FR, and the electron-hole Coulomb attraction U_{eh} . The latter is relevant only in the final configuration, where it effectively lowers the electron level energy to $\varepsilon - U_{eh}$, thus ensuring the double occupancy of the electron level in the final

configuration. A Hartree-Fock estimate from the PL data in Figure 1b yields $U_{\text{eh}} \simeq U_{\text{ee}} + 4 \text{ meV}$.

Absorption line shape. The inset of Figure 2a shows high resolution laser absorption spectroscopy on the same QD across the X^- single electron charging plateau (see Supporting Online Material). Here, we parameterize V_g in terms of ε , normalized and shifted such that $\varepsilon = -\frac{1}{2}U_{\text{ee}}$ for the gate voltage where the absorption contrast is maximal. Instead of the usual linear dc-Stark shift of the absorption peak that is characteristic of charge-tunable QDs, we find a strongly non-linear ε -dependent shift of the X^- transition energy [7, 8], which measures the energy difference between the final and initial ground states. This energy shift arises from a renormalization of the initial state energy [22] due to virtual tunneling between the singly-occupied QD and FR (analogous to the Lamb shift of atomic ground states). The final trion state energy, on the other hand, is hardly affected by virtual tunneling processes, due to large $U_{\text{eh}} - U_{\text{ee}}$. As depicted in Figure 2c and explained in its caption, this renormalization-induced red-shift of the initial state is strongest at the plateau edges and leads to an ε -dependent blue-shift of the optical resonance frequency. The latter can be used to determine the EAM model parameters: $U_{\text{ee}}=7.5 \text{ meV}$, $\Gamma = 0.7 \text{ meV}$, and $D = 3.5 \text{ meV}$. NRG calculations for the transition energy (Figure 2a, solid blue line) give excellent agreement with the experimental data (blue symbols).

Figure 3a shows on a log-log scale, the blue tail of the normalized absorption line shapes, where the applied laser frequency is larger than the transition energy, for the four values of gate voltage indicated by arrows in inset of Figure 2a. Inset to Figure 3a compares the full unnormalized absorption line shapes for the identical gate voltages in linear scale; the red absorption tail allows us to determine the temperature of the FR as $T_{\text{FR}} = 180 \text{ mK} = 15.6 \mu\text{eV}$ (see Supporting Online Material). The strong variation of the peak absorption strength in Figure 3a inset is a consequence of the exponential dependence of the Kondo temperature $T_{\text{K}}(\varepsilon) = \sqrt{\Gamma D} e^{-[1-(2\varepsilon/U_{\text{ee}}+1)^2](\pi U_{\text{ee}}/8\Gamma)}$ on the gate voltage ε . For this QD, T_{K} varies between $24 \mu\text{eV}$ and $464 \mu\text{eV}$ [27]. All line shapes carry the signatures of an optical interference effect induced by the sample structure (causing some lineshapes to become negative for small red detunings), and of independently measured fluctuations in gate voltage; both effects have been taken into account in the calculated line shapes (see Supporting Online Material). Calculating the line shapes by NRG (solid lines) without any further fit parameters, we find remarkable agreement with experiment for all four lineshapes depicted in Fig. 3a, demonstrating the validity of the excitonic Anderson Model [23] for the coupled QD-FR system.

Perturbative regime. To obtain better insight into the underlying physics, we first consider the absorption line shape for blue detunings satisfying $\nu >$

$\max(T_{\text{FR}}, T_{\text{K}})$, where a perturbative description is possible. All four line shapes in Fig. 3a impressively show the ν^{-1} dependence expected for the perturbative regime. The origin of the ν^{-1} tail can be understood as arising from a two-step process, where a virtual excitation of a valence-band electron to the conduction band is followed by excitation of an electron-hole pair in the FR via an effective spin-exchange coupling. The energy of the electron-hole pair is equal to ν , ensuring energy conservation. The lowest-energy electron in the FR, which can contribute to this process, has an energy $-\nu$ (we took the Fermi energy to be 0). Assuming a constant density of states around the Fermi level of the FR, the effective bandwidth of electrons contributing to this two-step absorption process at a detuning ν is equal to ν . The electron-hole pair generation therefore contributes an additional phase space factor $\propto \nu$ to the Lorentzian broadened QD trion transition [23], such that the overall lineshape has approximately a $1/\nu$ tail.

Scaling collapse. For gate voltages such that the initial ground state is a Kondo singlet, the absorption line shape, normalized to its value at $\nu = T_{\text{K}}$, is expected [23] to be a universal function of ν/T_{K} in the regime $T_{\text{FR}} \ll \nu \ll U_{\text{ee}}$. To confirm this prediction, Fig. 3c shows $A(\nu)/A(T_{\text{K}}(\varepsilon))$ as a function of ν/T_{K} for three of the line shapes of Fig. 3a (but omitting the black one, for which the coupled system is in the mixed valence regime). A striking scaling collapse is evident [28]. Multiplying T_{K}

by a constant factor ξ for all three ε values yields a scaling collapse of nearly identical quality, provided $1 \leq \xi \leq 5$. This reflects the fact that T_{K} , being a crossover scale, is defined only up to an arbitrary pre-factor of order one.

Strong-coupling Kondo regime. In the limit $T_{\text{FR}} < \nu < T_{\text{K}}$, a perturbative description of the lineshape is no longer valid. In the initial configuration, the exchange interaction between QD and FR induces a *Kondo screening cloud* that forms a singlet with the QD spin. This acts as a scattering potential that induces *strong* phase shifts for those low-energy fermionic excitations whose energies are within T_{K} from the Fermi level. In the final configuration after photon absorption, the QD has two electrons in a *local* singlet state. Therefore the Kondo screening cloud, and the scattering potential for FR electrons constituted by it, disappear in the long time limit: the corresponding ground state wave-function is a tensor product of the local singlet and free electronic states, with only *weak* phase shifts. Since the initial and final FR phase shifts differ (as depicted schematically in Fig. 2d), the FR does not remain a spectator during the X^- transition: instead, the transition matrix element between the ground states of the initial and final configurations is vanishingly small. This leads to an AOC which manifests itself by transforming a delta-function resonance (of an uncoupled QD) into a power-law singularity [15] of the form $\nu^{-\eta}$, where the exponent η characterizes the extent of AOC. For $T_{\text{FR}} \ll \nu \ll T_{\text{K}}$, the

absorption lineshape of the X^- transition is expected to show an analogous power-law singularity. The exponent η is predicted [23, 24] to range between 0 and 0.5 (assuming no magnetic field), with $\eta \simeq 0.5$ being characteristic for a Kondo-correlated initial state and an uncorrelated final state. This lineshape modification is a consequence of a redistribution of the optical oscillator strength, associated with the fact that the FR wave-function in the Kondo correlated initial state has finite overlap with a range of final states consisting of electron-hole pair excitations out of a non-interacting FR.

If $T_{\text{FR}} \ll T_K$ and the optical detuning is reduced below T_K , the lineshape is predicted to smoothly cross over from the perturbative $1/\nu$ tail to the strong-coupling AOC $1/\nu^{0.5}$ power law just discussed. This crossover is illustrated in Fig. 3b (dashed lines) by NRG calculations, performed at $T_{\text{FR}} = 0$ for the four ε -values of Fig. 3a: Remarkably, despite drastic differences in the $\nu > T_K$ tails due to different values of $T_K(\varepsilon)$, all four lineshapes show similar power-law exponents around $\eta \simeq 0.5$ for $\nu \ll T_K$, in accordance with predictions [23] based on Hopfield's rule (see Supplementary Information). For nonzero temperature, however, the $1/\nu^{0.5}$ power law is cut off and saturates once ν decreases past T_{FR} (Fig. 3b, solid lines), because of thermal averaging over initial states with excitation energies $\lesssim T_{\text{FR}}$.

Magnetic field-tuning of Kondo correlations. A direct extraction of the $1/\nu^{0.5}$ power law from the mea-

sured data is difficult due to the small accessible experimental window $T_{\text{FR}} < \nu < T_K$. Nevertheless, we are able to determine the power-law exponent corresponding to our data accurately by using the fact that the detailed form of the line shape sensitively depends on the exponent η which can be tuned by an external magnetic field[23]. Figure 4a shows the measured absorption line shape of a second QD at $B_{\text{ext}} = 0$ Tesla (black squares) and the line shapes of the blue (blue dots) and red (red triangles) Zeeman/trion transition at $B_{\text{ext}} = 1$ Tesla in a linear scale. We have determined the parameters of this QD to be $U_{\text{ee}} = 7.5$ meV, $\Gamma = 1$ meV, $D = 6.5$ meV and $U_{\text{eh}} = 3/2U_{\text{ee}}$; the data were taken at $T_{\text{FR}} = 15.6\mu\text{eV}$ for $\varepsilon/U_{\text{ee}} = -0.43$ where $T_K = 140\mu\text{eV}$. While the peak contrast at $B_{\text{ext}} = 1$ Tesla for the blue (red) trion transition increases (decreases) by a factor ~ 2 , the area under the absorption curve increases (decreases) by less than 20%; this observation proves that the change in the line shape is predominantly due to a line narrowing associated with a increase (decrease) of the power-law exponent η . Conversely, the small change in the area under the absorption curve despite having $B_{\text{ext}} = 2.5T_{\text{FR}}$ demonstrates that the initial state is a Kondo singlet that suppresses the electron Zeeman splitting. The inset to Fig. 4a shows the B_{ext} dependence of the peak absorption contrast for the blue and red trion transitions; while the agreement with the predictions of NRG is excellent for $B_{\text{ext}} \leq 1.5$ Tesla, the blue trion contrast exhibits oscilla-

tions for higher B_{ext} ; this is most likely a consequence of the modification of the FR density of states at high fields in Faraday configuration. Fig. 4b shows the normalized line shape in a log-log plot together with the results of the NRG calculation (solid lines): η values that we determine from these plots range from 0.31 (red trion) to 0.66 (blue trion), and prove the sensitivity of the measured line shapes to the AOC determined power-law exponents. These experiments unequivocally demonstrate the magnetic tuning of the AOC exponent for the first time.

The remarkable agreement between our experimental data depicted in Figs.2-4 and the NRG calculations clearly demonstrate Kondo correlations between a QD electron and the electrons in a FR, as predicted by the excitonic Anderson model. The optical probe of these correlations unequivocally show the signatures of Anderson orthogonality physics associated with the quantum quench of Kondo correlations. Our experiments establish the potential of single optically active QDs in investigating many-body physics. In addition, they pave the way for a new class of quantum optics experiments where the influence of simultaneous presence of non-perturbative coherent cavity/laser coupling and Kondo correlations on electric field and photon correlations could be investigated.

-
- [1] Michler, P. *et al.*, A Quantum Dot Single-Photon Turnstile Device. *Science*, **290**, 2282-2285 (2000).
- [2] Dousse, A. *et al.*, Ultrabright source of entangled photon pairs. *Nature*, **466**, 217-220 (2010).
- [3] Press, D., Ladd, T. D., Zhang, B., Yamamoto, Y., Complete quantum control of a single quantum dot spin using ultrafast optical pulses. *Nature*, **456**, 218-221 (2008).
- [4] Kim, D., Carter, S. G., Greilich, A., Bracker, A., Gammon, D., Ultrafast optical control of entanglement between two quantum dot spins. arXiv:1007.3733
- [5] Yilmaz, S. T., Fallahi, P., Imamoglu, A. Quantum-Dot-Spin Single-Photon Interface. *Phys. Rev. Lett.*, **105**, 033601 (2010)
- [6] Claassen, M., Türeci, H., Imamoglu, A., Solid-State Spin-Photon Quantum Interface without Spin-Orbit Coupling. *Phys. Rev. Lett.*, **104**, 177403 (2010)
- [7] Dalgarno, P. A., *et al.*, Optically Induced Hybridization of a Quantum Dot State with a Filled Continuum. *Phys. Rev. Lett.*, **100**, 176801 (2008)
- [8] Kleemans, N. A. J. M. *et al.*, Many-body exciton states in self-assembled quantum dots coupled to a Fermi sea. *Nature Physics*, **6**, 534-538, (2010)
- [9] Latta, C. *et al.*, Confluence of resonant laser excitation and bidirectional quantum-dot nuclear-spin polarization. *Nature Physics*, **5**, 758-763 (2009)
- [10] Xu, X. *et al.*, Optically controlled locking of the nuclear field via coherent dark-state spectroscopy. *Nature*, **459**, 1105-1109, (2009)
- [11] Högele, A. *et al.*, Voltage-Controlled Optics of a Quantum Dot. *Phys. Rev. Lett.*, **93**, 217401 (2004).
- [12] Kondo, J., Resistance Minimum in Dilute Magnetic Alloys. *Progress of Theoretical Physics*, **32**, 37 (1964).
- [13] Kouwenhoven, L. P., Glazman, L., Revival of the Kondo effect. *Physics World*, **14**, 33 (2001).
- [14] Atatüre, M. *et al.*, Quantum-Dot Spin-State Preparation with Near-Unity Fidelity. *Science* **312**, 551-553 (2006).
- [15] Mahan, G. *Many-Particle Physics*, Kluwer Academic(New York), 2000.
- [16] Anderson, P. W., Infrared Catastrophe in Fermi Gases with Local Scattering Potentials. *Phys. Rev. Lett.*, **18**, 1049-1051 (1967)
- [17] Goldhaber-Gordon, D. *et al.*, Kondo effect in a single-electron transistor. *Nature*, **391**, 156-159 (1998).
- [18] Cronenwett, S. M., Oosterkamp, T. H., Kouwenhoven, L. P., A Tunable Kondo Effect in Quantum Dots. *Science*, **281**, 540 (1998).
- [19] van der Wiel, W. G. *et al.*, The Kondo Effect in the Unitary Limit. *Science*, **289**, 2105-2108, (2000)
- [20] Warburton, R. J. *et al.*, Optical emission from a charge-tunable quantum ring. *Nature*, **405**, 926-929, (2000)
- [21] Govorov, A. O., Karrai, K. Warburton, R. J., Kondo excitons in self-assembled quantum dots. *Phys. Rev. B*, **67**, 241307 (2003).
- [22] Anderson, P. W., Localized Magnetic States in Metals *Phys. Rev.*, **124**, 41-53 (1961)
- [23] Türeci, H. E. *et al.*, Shedding light on non-equilibrium dynamics of a spin coupled to fermionic reservoir. arXiv:0907.3854
- [24] Helmes, R. W., Sindel, M., Borda, L., von Delft, J., Absorption and emission in quantum dots: Fermi surface effects of Anderson excitons. *Phys. Rev. B*, **72**, 125301 (2005).
- [25] Goldhaber-Gordon, D. *et al.*, From the Kondo Regime to the Mixed-Valence Regime in a Single-Electron Transistor. *Phys. Rev. Lett.* **81**, 5225 (1998)
- [26] Hopfield, J. J., *Comments on Sol. St. Phys.*, **II**, 2 (1969).
- [27] T_K loses significance for the black curve, for which the QD-FR system is in the mixed-valence regime.
- [28] Deviations from scaling for $\nu < T_{FR}$ are expected, but masked by an insufficiently small signal-to-noise ratio of the experimental data.

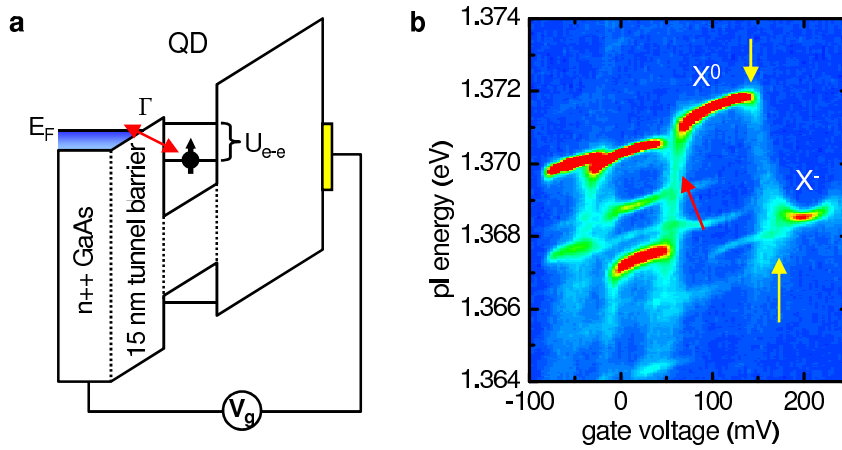


Figure 1: A single quantum dot strongly coupled to a fermionic reservoir. (a) Band structure of the device. The QDs are separated by a 15 nm tunnel barrier from a n^{++} -doped GaAs layer (Fermi sea). A voltage V_g applied between the electron gas and a semi-transparent NiCr gate on the sample surface controls the relative value of the QD single-particle energy levels with respect to the Fermi energy E_F . (b) Low temperature (4 K) photoluminescence spectrum of a single QD as a function of V_g . The interaction of the QD electron with the Fermi sea leads to a broadening of the photoluminescence lines at the plateau edges (yellow arrows) and indirect recombinations of a QD hole and a Fermi sea electron (red arrow). Indirect transitions are identified by the stronger V_g dependence of the transition energy compared to direct transitions.

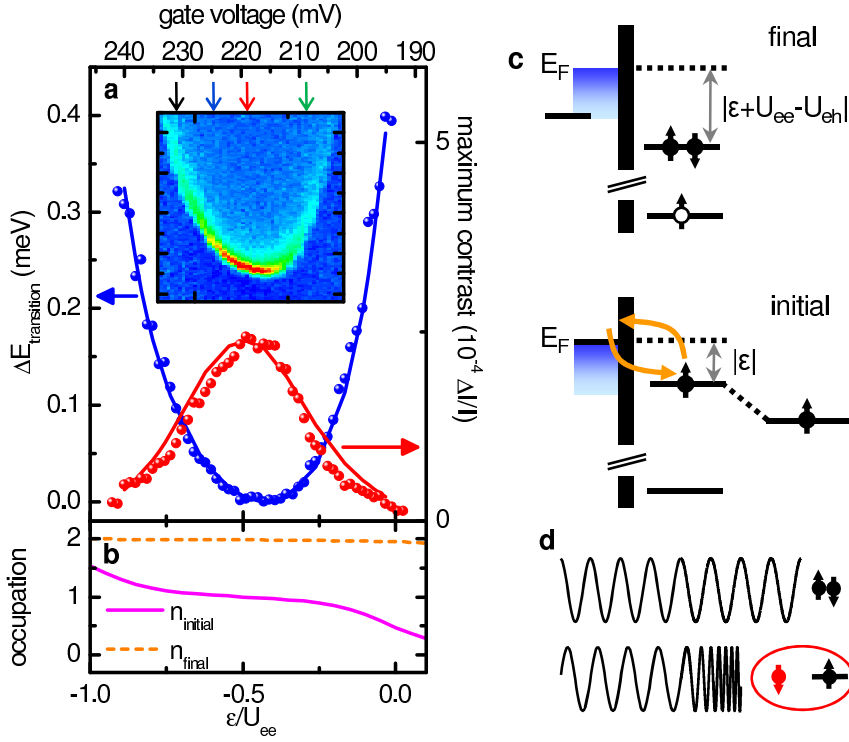


Figure 2: The gate voltage dependence of the peak absorption strength of the negatively charged exciton X^- , measured at 180 mK. (a) Inset: absorption as a function of the gate voltage. Main figure: Experimental data (symbols) for the ϵ -dependence of the shift in the resonance energy $\Delta E_{\text{transition}}$ (blue, left axis) and the absorption contrast (red, right axis) are well reproduced by NRG calculations (solid lines) for the following parameters: $U_{ee} = 7.5$ meV, $\Gamma = 0.7$ meV, $D = 3.5$ meV, $U_{eh} = 11$ meV, $T_{\text{FR}} = 180$ mK. (b) Lower panel: NRG results for the occupancy of the QD electron level in the initial and final ground states. (c) Schematic of the energy renormalization process: The initial configuration (bottom) features a single electron in the QD, whose energy is lowered by virtual tunneling between QD and FR. Since virtual excitations with energy ΔE contribute a shift proportional to $-\Gamma/\Delta E$, the total shift (involving a sum over all possible ΔE), is strongest near the edges of the X^- plateau. Toward the right edge (ϵ near 0), the dominant contribution comes from virtual tunneling of the QD electron into the FR (as depicted); toward the left edge (ϵ near $-U_{ee}$), it comes from virtual tunneling of a FR electron into the QD (not depicted). In the final configuration (top), the QD contains two electrons and a hole. The electron-hole Coulomb attraction U_{eh} effectively lowers the QD electron level energy to $\epsilon - U_{eh}$. This raises the energy costs ΔE for virtual excitations by $U_{eh} - U_{ee}$ (which is $\gg \Gamma$), so that final state energy renormalization is negligible. The renormalization of the transition energy (red arrow), probed by a weak laser, is thus mainly due to initial state energy renormalization. (d) Cartoon for Anderson orthogonality: the Kondo cloud (bottom) and local singlet (top) of the initial and final configurations produce strong or weak phase shifts, respectively.

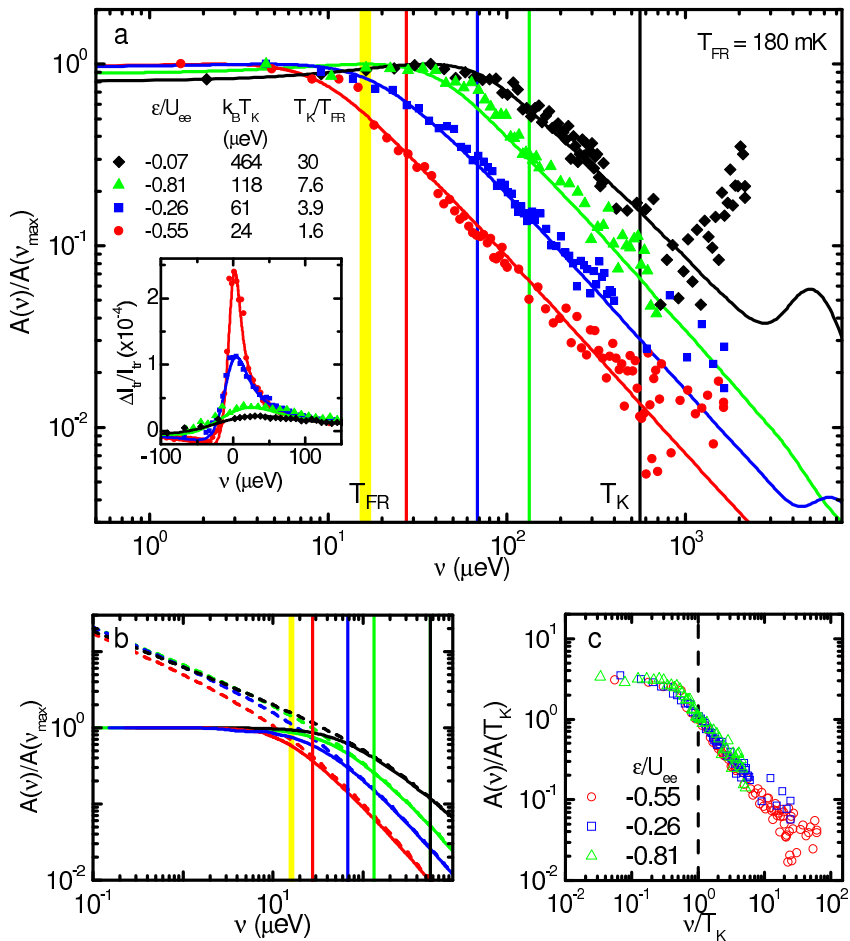


Figure 3: The absorption line shape $A(\nu)$. **a** The blue tail of $A(\nu)/A(\nu_{\max})$, plotted versus the laser detuning ν on a log-log scale. The experimental data were taken at an electron temperature of $T_{\text{FR}} = 180$ mK for the four values of gate voltage (ε) indicated by arrows in Fig. 2a; the corresponding Kondo temperatures $T_{\text{K}}(\varepsilon)$ are indicated by vertical lines in matching colors. NRG results (solid lines), obtained using the parameters from the fit in Fig. 2a, are in remarkable agreement with experiment. Inset: the measured full (unnormalized) absorption line shape in linear scale for the identical ε values. **b**, NRG results for $T = T_{\text{FR}}$ and $T = 0$; the latter show the $\nu^{-0.5}$ behaviour expected in the strong-coupling regime, $T \ll \nu \ll T_{\text{K}}$. **c**, The rescaled lineshape $A(\nu)/A(\nu_{\max})$ versus ν/T_{K} shows a universal scaling collapse characteristic of Kondo physics.

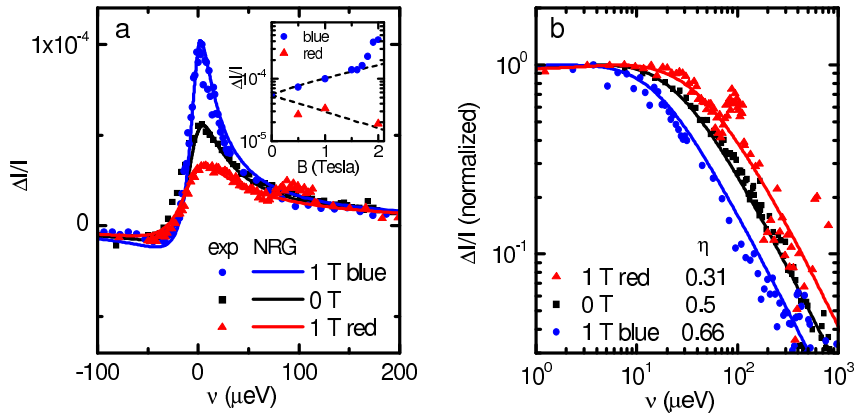


Figure 4: Magnetic field dependence of the absorption. (a) The absorption line shapes for a second QD with similar parameters (see text) for $\varepsilon = -0.43$ at $B_{ext} = 0$ Tesla and $B_{ext} = 1$ Tesla for the blue/red trion transition. The magnetic field changes the strength of the AOC and the lineshape. Inset: the peak absorption contrast showing good agreement with the NRG calculations for $B \leq 1.5$ Tesla. (b) The normalized absorption line shape in a log-log plot. These measurements pin the value of $\eta(B_{ext} = 0)$ to ~ 0.5 - a direct signature of a Kondo singlet in the absorption lineshape. In addition they demonstrate the tunability of an orthogonality exponent.